Structure-preserving strategy for conservative simulation of the relativistic nonlinear Landau-Fokker-Planck equation

Takashi Shiroto* and Yasuhiko Sentoku†
Institute of Laser Engineering, Osaka University, Suita, Osaka 565-0871, Japan

(Received 21 February 2019; published 28 May 2019)

Mathematical symmetries of the Beliaev-Budker kernel are the most important structure of the relativistic Landau-Fokker-Planck equation. In most numerical simulations, however, one of the symmetries is not preserved in the discrete level resulting in a violation of the energy conservation. Recently, we proposed a charge-momentum-energy-conserving relativistic Vlasov-Maxwell scheme by preserving mathematical formulas in discrete form, and here we apply the concept to the relativistic Landau-Fokker-Planck equation. Through a numerical experiment of relativistic collisional relaxation, a mass-momentum-energy-conserving simulation has been demonstrated without any artificial constraints.

DOI: 10.1103/PhysRevE.99.053309

I. INTRODUCTION

Collisional processes of relativistic plasmas are essential in fusion and astrophysical plasmas. In fast ignition of the inertial confinement fusion [1], relativistic electron beams are generated with short-pulse lasers and heat a high-density fuel core through collisional processes. Such a relativistic physics is also crucial to suppression of runaway electrons generated in tokamak disruption [2]. Relativistic electrons up to 100 MeV would damage plasma facing components especially in large tokamaks [3]. Furthermore, power-law spectrum generation has been a great interest in astrophysics for decades. For example, Fermi acceleration [4] is regarded as an origin of energetic cosmic rays, but observed spectra have not been reproduced by numerical simulations accurately. Such stochastic collisional physics is described by the Landau-Fokker-Planck (LFP) equation.

The LFP equation in the International System of Units is [5]

$$\frac{\partial f_s}{\partial t} = \frac{\Gamma}{2m_s^2}\frac{\partial}{\partial \mathbf{u}} \cdot \int \mathsf{U}(\mathbf{u},\mathbf{u}') \cdot \left(f_{s'}\frac{\partial f_s}{\partial \mathbf{u}} - \frac{m_s}{m_{s'}} f_s \frac{\partial f_{s'}}{\partial \mathbf{u}'} \right) d\mathbf{u}', \tag{1}$$

where $\Gamma = (q_s^2 q_{s'}^2 \log\Lambda)/4\pi\varepsilon_0{}^2$, $\log\Lambda$ is the Coulomb logarithm, ε_0 is the vacuum permittivity, $(f_s, f_{s'})$, $(m_s, m_{s'})$, $(q_s, q_{s'})$, and $(\mathbf{u}, \mathbf{u}')$ are the distribution function, mass, electric charge, and momentum per unit mass of species (s, s'), respectively. In the relativistic case, the Beliaev-Budker kernel $\mathsf{U}(\mathbf{u},\mathbf{u}')$ is described as follows [6]:

$$\mathsf{U} = \frac{r^2}{\gamma\gamma' w^3}[w^2\mathsf{I} - \gamma^2\mathbf{v}\mathbf{v} - \gamma'^2\mathbf{v}'\mathbf{v}' + r\gamma\gamma'(\mathbf{v}\mathbf{v}' + \mathbf{v}'\mathbf{v})], \tag{2}$$

where $r = \gamma\gamma'(1 - \mathbf{v}\cdot\mathbf{v}'/c^2)$, $w = c\sqrt{r^2-1}$, $\mathbf{v} = \mathbf{u}/\gamma$, $\mathbf{v}' = \mathbf{u}'/\gamma'$, and c is the speed of light in vacuum. The Lorentz factor is defined as follows:

$$\gamma = \sqrt{1 + |\mathbf{u}/c|^2} = 1/\sqrt{1 - |\mathbf{v}/c|^2}, \tag{3}$$

$$\gamma' = \sqrt{1 + |\mathbf{u}'/c|^2} = 1/\sqrt{1 - |\mathbf{v}'/c|^2}. \tag{4}$$

The relativistic LFP equation is designed so as to ensure the mass-momentum-energy conservation and the H-theorem.

In practical simulations, the relativistic LFP equation is often linearized so that the computational cost is reduced from $O(N^2)$ to $O(N)$, where N is the number of unknowns. For fast ignition, a linearization of Nakashima and Takabe [7] is employed by relativistic Fokker-Planck codes such as RFP-2D [8], FIBMET [9], and FIDO [10,11]. The linearization is based on the fact that the colliding particles are much faster than the collided ones. This violates symmetry of the collision kernel so the conservation laws are maintained only at the continuous limit. For runaway electrons in tokamak disruptions, linearization which assumes a weakly relativistic equilibrium background [12,13] is sometimes performed to take into account the effect of nonthermal electrons [14], while the conservation laws are violated. Further, TASK/FP [15] and CQL3D [16] codes have options that decompose the nonlinear LFP equation into Legendre modes and solve first a few modes. The Legendre polynomials ensure the mass-momentum-energy conservation but limit resolving structures of the pitch angle. Recently, Stahl *et al.* developed the NORSE code [17], which models nonlinear electron-electron collisions by the Braams-Karney potential formulation [18]. However, the NORSE code violates the conservation laws including the mass conservation. In the potential form, the "nonlinear constraints" is one of the ways to preserve the conservation laws [19] and equilibrium state [20], i.e., one of the projection methods in the literature of applied mathematics [21]. However, the projection method can affect the stability of numerical schemes, and it may not be suited for long timescale simulations. In magnetohydrodynamics

*Present address: National Institutes for Quantum and Radiological Science and Technology, Rokkasho, Aomori 039-3212, Japan; shiroto.takashi@qst.go.jp
†sentoku-y@ile.osaka-u.ac.jp

simulations, for example, the projection method [22] or constrained transport method [23] has been used to enforce the solenoidal constraint ($\nabla \cdot \mathbf{B} = 0$). However, such an inconsistent magnetic field can induce a "checkerboard phenomenon," which is one of the numerical instabilities [24].

Unlike the relativistic regime, many nonrelativistic structure-preserving schemes have been proposed to ensure the conservation laws, positivity, and H-theorem. Chang and Cooper developed a positivity-preserving scheme for the one-dimensional (1D) linearized LFP equation [25], and it was extended to the nonlinear isotropic LFP equation [26] and nonlinear multidimensional one [27–29] preserving the conservation laws and H-theorem. A structure-preserving finite-element scheme [30] is also developed to ensure the conservation laws on unstructured meshes. These works are based on a weak form associated with Eq. (1). The integrand of Eq. (1) can be transformed into the following one analytically:

$$f_s f_{s'} \mathsf{U}(\mathbf{u}, \mathbf{u}') \cdot \left(\frac{\partial \log f_s}{\partial \mathbf{u}} - \frac{m_s}{m_{s'}} \frac{\partial \log f_{s'}}{\partial \mathbf{u}'} \right). \tag{5}$$

The weak form coming from Eq. (5) is called the "log" weak-form, and the proof of the H-theorem by the log weak form is straightforward. An analytical discussion was first given by Pekker and Khudik [31], and conservative and entropic discretizations have been proposed for isotropic [32,33] and multidimensional cases [34,35]. Furthermore, an energy-conserving LFP scheme with the Rosenbluth potential form [36] was proposed using an analogy of the Maxwell stress tensor in electromagnetism [37,38]. However, structure-preserving schemes for the relativistic LFP equation have not been developed since the Lorentz factor is not expressed as polynomials of finite order in the momentum [30].

In this paper, we demonstrate a structure-preserving simulation of the relativistic LFP equation which strictly preserves the conservation laws of mass, momentum, and energy. The key concept is the same with our recent work about a quadratic conservative scheme for the relativistic Vlasov-Maxwell system [39]. The previous paper states that mathematical formulas such as the product rule must be treated carefully to maintain the conservation laws in discrete forms, and we reveal that the same way of thinking can be extended to the relativistic LFP equation. Moreover, a similar approach has been used in a nonrelativistic scheme with nonuniform meshes [40,41]. The rest of this paper is composed as follows. Section II shows an intuitive discretization which cannot maintain the energy conservation. Section III deductively derives requirements for the conservation laws in discrete form. Our structure-preserving scheme and its concept are introduced in Sec. IV. A verification of conservation property through a thermal-equilibration is performed in Sec. V. Section VI gives the conclusions of this article.

II. CONVENTIONAL SCHEME

In this article, the relativistic LFP equation is discretized as follows. Note that the conservation laws are not affected by the temporal structure, so only momentum dimensions are discretized here:

$$\frac{\partial f_s^{\mathbf{j}}}{\partial t} \equiv \frac{\Gamma}{2m_s{}^2} \frac{\delta}{\delta \mathbf{u}} \cdot \sum_{\mathbf{k}} \mathsf{U}(\mathbf{u}^{\mathbf{j}}, \mathbf{u}'^{\mathbf{k}}) \cdot \left(f_{s'}{}^{\mathbf{k}} \frac{\delta f_s^{\mathbf{j}}}{\delta \mathbf{u}} - \frac{m_s}{m_{s'}} f_s^{\mathbf{j}} \frac{\delta f_{s'}{}^{\mathbf{k}}}{\delta \mathbf{u}'} \right) \Delta \mathbf{u}', \tag{6}$$

where $\mathbf{j} \equiv [j_1, j_2, j_3]$ and $\mathbf{k} \equiv [k_1, k_2, k_3]$ are the indices of uniform momentum grids for $\mathbf{u}$ and $\mathbf{u}'$, respectively. $\Delta \mathbf{u} \equiv \Delta u_1 \Delta u_2 \Delta u_3$, and $(\Delta u_1, \Delta u_2, \Delta u_3)$ is the grid interval of (u_1, u_2, u_3). The species (s, s′) use the same momentum grids ($\mathbf{u}^{\mathbf{j}} = \mathbf{u}'^{\mathbf{j}}$, $\Delta \mathbf{u} = \Delta \mathbf{u}'$). Here we use a second-order central difference for simplicity:

$$\begin{aligned}
\frac{\delta a^{\mathbf{j},\mathbf{k}}}{\delta u_1} &\equiv \frac{a^{j_1+1,j_2,j_3,k_1,k_2,k_3} - a^{j_1-1,j_2,j_3,k_1,k_2,k_3}}{2\Delta u_1}, \\
\frac{\delta a^{\mathbf{j},\mathbf{k}}}{\delta u_2} &\equiv \frac{a^{j_1,j_2+1,j_3,k_1,k_2,k_3} - a^{j_1,j_2-1,j_3,k_1,k_2,k_3}}{2\Delta u_2}, \\
\frac{\delta a^{\mathbf{j},\mathbf{k}}}{\delta u_3} &\equiv \frac{a^{j_1,j_2,j_3+1,k_1,k_2,k_3} - a^{j_1,j_2,j_3-1,k_1,k_2,k_3}}{2\Delta u_3}, \\
\frac{\delta a^{\mathbf{j},\mathbf{k}}}{\delta u'_1} &\equiv \frac{a^{j_1,j_2,j_3,k_1+1,k_2,k_3} - a^{j_1,j_2,j_3,k_1-1,k_2,k_3}}{2\Delta u'_1}, \\
\frac{\delta a^{\mathbf{j},\mathbf{k}}}{\delta u'_2} &\equiv \frac{a^{j_1,j_2,j_3,k_1,k_2+1,k_3} - a^{j_1,j_2,j_3,k_1,k_2-1,k_3}}{2\Delta u'_2}, \\
\frac{\delta a^{\mathbf{j},\mathbf{k}}}{\delta u'_3} &\equiv \frac{a^{j_1,j_2,j_3,k_1,k_2,k_3+1} - a^{j_1,j_2,j_3,k_1,k_2,k_3-1}}{2\Delta u'_3},
\end{aligned}$$

where $a^{\mathbf{j},\mathbf{k}} \equiv a(\mathbf{u}^{\mathbf{j}}, \mathbf{u}'^{\mathbf{k}})$ is an arbitrary function.

In an intuitive discretization, the collision kernel is calculated by its arguments directly:

$$\mathsf{U}(\mathbf{u}^{\mathbf{j}}, \mathbf{u}'^{\mathbf{k}}) \equiv \frac{(r^{\mathbf{j},\mathbf{k}})^2}{\gamma^{\mathbf{j}} \gamma'^{\mathbf{k}} (w^{\mathbf{j},\mathbf{k}})^3} [(w^{\mathbf{j},\mathbf{k}})^2 \mathsf{I} - \mathbf{u}^{\mathbf{j}} \mathbf{u}^{\mathbf{j}} - \mathbf{u}'^{\mathbf{k}} \mathbf{u}'^{\mathbf{k}} + r^{\mathbf{j},\mathbf{k}} (\mathbf{u}^{\mathbf{j}} \mathbf{u}'^{\mathbf{k}} + \mathbf{u}'^{\mathbf{k}} \mathbf{u}^{\mathbf{j}})]. \tag{7}$$

From the definition, the collision kernel Eq. (7) satisfies two mathematical symmetries:

$$\mathsf{U}(\mathbf{u}^{\mathbf{j}}, \mathbf{u}'^{\mathbf{k}}) = \mathsf{U}(\mathbf{u}'^{\mathbf{k}}, \mathbf{u}^{\mathbf{j}}), \tag{8}$$

$$\mathsf{U}(\mathbf{u}^{\mathbf{j}}, \mathbf{u}'^{\mathbf{k}}) \cdot \mathbf{v}^{\mathbf{j}} = \mathsf{U}(\mathbf{u}'^{\mathbf{k}}, \mathbf{u}^{\mathbf{j}}) \cdot \mathbf{v}'^{\mathbf{k}}. \tag{9}$$

III. REQUIREMENTS FOR CONSERVATION LAWS IN DISCRETE FORM

In this section, requirements for the conservation laws are derived deductively. The mass conservation is trivially maintained, so the discussion is focused on the momentum-energy conservation. The following points are required to prove the conservation laws analytically from the relativistic LFP equation:

(1) Integration-by-parts must be maintained.

(2) $\mathsf{U}(\mathbf{u}, \mathbf{u}') = \mathsf{U}(\mathbf{u}', \mathbf{u})$ is required for the momentum conservation.

(3) $\mathsf{U}(\mathbf{u}, \mathbf{u}') \cdot \mathbf{v} = \mathsf{U}(\mathbf{u}', \mathbf{u}) \cdot \mathbf{v}'$ is required for the energy conservation.

If one can assume $a^{\mathbf{j},\mathbf{k}} = 0$ at the momentum boundaries, the following summation-by-parts, i.e., the integration-by-parts in discrete form, is valid:

$$\sum_{\mathbf{j},\mathbf{k}} \left(\frac{\delta a^{\mathbf{j},\mathbf{k}}}{\delta \mathbf{u}} b^{\mathbf{j},\mathbf{k}} \right) \Delta\mathbf{u}\Delta\mathbf{u}' = -\sum_{\mathbf{j},\mathbf{k}} \left(a^{\mathbf{j},\mathbf{k}} \frac{\delta b^{\mathbf{j},\mathbf{k}}}{\delta \mathbf{u}} \right) \Delta\mathbf{u}\Delta\mathbf{u}',$$

$$\sum_{\mathbf{j},\mathbf{k}} \left(\frac{\delta a^{\mathbf{j},\mathbf{k}}}{\delta \mathbf{u}'} b^{\mathbf{j},\mathbf{k}} \right) \Delta\mathbf{u}\Delta\mathbf{u}' = -\sum_{\mathbf{j},\mathbf{k}} \left(a^{\mathbf{j},\mathbf{k}} \frac{\delta b^{\mathbf{j},\mathbf{k}}}{\delta \mathbf{u}'} \right) \Delta\mathbf{u}\Delta\mathbf{u}',$$

where $b^{\mathbf{j},\mathbf{k}}$ is also an arbitrary function. Therefore, the first point is automatically preserved if a finite-difference operator has a linearity. In addition, the second point is naturally satisfied unless the Braams and Karney potential is employed. The most important discussion in our article is the third point. To satisfy $a^{\mathbf{j},\mathbf{k}} = 0$ in the relativistic LFP equation, the computational domain must be large enough to ensure that the distribution function is negligible small at the boundary. In other words, no boundary condition can enforce all of the conservation laws.

A. Momentum conservation

The momentum of species "s" is described as a first-order moment of Eq. (6):

$$\begin{aligned}\frac{\partial}{\partial t}\left(\sum_{\mathbf{j}} m_{\mathrm{s}}\mathbf{u}^{\mathbf{j}} f_{\mathrm{s}}{}^{\mathbf{j}}\Delta\mathbf{u}\right) &= \frac{\Gamma}{2m_{\mathrm{s}}}\sum_{\mathbf{j}}\left[\mathbf{u}^{\mathbf{j}}\frac{\delta}{\delta\mathbf{u}}\cdot\sum_{\mathbf{k}}\mathsf{U}(\mathbf{u}^{\mathbf{j}},\mathbf{u}'^{\mathbf{k}})\cdot\left(f_{\mathrm{s}'}{}^{\mathbf{k}}\frac{\delta f_{\mathrm{s}}{}^{\mathbf{j}}}{\delta\mathbf{u}} - \frac{m_{\mathrm{s}}}{m_{\mathrm{s}'}}f_{\mathrm{s}}{}^{\mathbf{j}}\frac{\delta f_{\mathrm{s}'}{}^{\mathbf{k}}}{\delta\mathbf{u}'}\right)\Delta\mathbf{u}'\right]\Delta\mathbf{u} \\ &= -\frac{\Gamma}{2}\sum_{\mathbf{j},\mathbf{k}}\left[\mathsf{U}(\mathbf{u}^{\mathbf{j}},\mathbf{u}'^{\mathbf{k}})\cdot\left(\frac{f_{\mathrm{s}'}{}^{\mathbf{k}}}{m_{\mathrm{s}}}\frac{\delta f_{\mathrm{s}}{}^{\mathbf{j}}}{\delta\mathbf{u}} - \frac{f_{\mathrm{s}}{}^{\mathbf{j}}}{m_{\mathrm{s}'}}\frac{\delta f_{\mathrm{s}'}{}^{\mathbf{k}}}{\delta\mathbf{u}'}\right)\right]\Delta\mathbf{u}\Delta\mathbf{u}' \\ &\quad (\because \delta\mathbf{u}^{\mathbf{j}}/\delta\mathbf{u} \text{ is an identity matrix.})\end{aligned} \tag{10}$$

Likewise, the momentum of species "s′" is obtained as follows:

$$\frac{\partial}{\partial t}\left(\sum_{\mathbf{k}} m_{\mathrm{s}'}\mathbf{u}'^{\mathbf{k}} f_{\mathrm{s}'}{}^{\mathbf{k}}\Delta\mathbf{u}'\right) = -\frac{\Gamma}{2}\sum_{\mathbf{j},\mathbf{k}}\left[\mathsf{U}(\mathbf{u}'^{\mathbf{k}},\mathbf{u}^{\mathbf{j}})\cdot\left(\frac{f_{\mathrm{s}}{}^{\mathbf{j}}}{m_{\mathrm{s}'}}\frac{\delta f_{\mathrm{s}'}{}^{\mathbf{k}}}{\delta\mathbf{u}'} - \frac{f_{\mathrm{s}'}{}^{\mathbf{k}}}{m_{\mathrm{s}}}\frac{\delta f_{\mathrm{s}}{}^{\mathbf{j}}}{\delta\mathbf{u}}\right)\right]\Delta\mathbf{u}\Delta\mathbf{u}'. \tag{11}$$

The temporal development of total momentum is obtained as a sum of Eqs. (10) and (11):

$$\frac{\partial}{\partial t}\left(\sum_{\mathbf{j}} m_{\mathrm{s}}\mathbf{u}^{\mathbf{j}} f_{\mathrm{s}}{}^{\mathbf{j}}\Delta\mathbf{u} + \sum_{\mathbf{k}} m_{\mathrm{s}'}\mathbf{u}'^{\mathbf{k}} f_{\mathrm{s}'}{}^{\mathbf{k}}\Delta\mathbf{u}'\right) = -\frac{\Gamma}{2}\sum_{\mathbf{j},\mathbf{k}}\left\{[\mathsf{U}(\mathbf{u}^{\mathbf{j}},\mathbf{u}'^{\mathbf{k}}) - \mathsf{U}(\mathbf{u}'^{\mathbf{k}},\mathbf{u}^{\mathbf{j}})]\cdot\left(\frac{f_{\mathrm{s}'}{}^{\mathbf{k}}}{m_{\mathrm{s}}}\frac{\delta f_{\mathrm{s}}{}^{\mathbf{j}}}{\delta\mathbf{u}} - \frac{f_{\mathrm{s}}{}^{\mathbf{j}}}{m_{\mathrm{s}'}}\frac{\delta f_{\mathrm{s}'}{}^{\mathbf{k}}}{\delta\mathbf{u}'}\right)\right\}\Delta\mathbf{u}\Delta\mathbf{u}'. \tag{12}$$

Therefore, the intuitive kernel of Eq. (7) strictly maintains the momentum conservation owing to Eq. (8).

B. Energy conservation

The energy of species "s" is described as a second-order moment of Eq. (6):

$$\begin{aligned}\frac{\partial}{\partial t}\left(\sum_{\mathbf{j}} m_{\mathrm{s}}c^2\gamma^{\mathbf{j}} f_{\mathrm{s}}{}^{\mathbf{j}}\Delta\mathbf{u}\right) &= \frac{\Gamma}{2m_{\mathrm{s}}}\sum_{\mathbf{j}}\left[\gamma^{\mathbf{j}}c^2\frac{\delta}{\delta\mathbf{u}}\cdot\sum_{\mathbf{k}}\mathsf{U}(\mathbf{u}^{\mathbf{j}},\mathbf{u}'^{\mathbf{k}})\cdot\left(f_{\mathrm{s}'}{}^{\mathbf{k}}\frac{\delta f_{\mathrm{s}}{}^{\mathbf{j}}}{\delta\mathbf{u}} - \frac{m_{\mathrm{s}}}{m_{\mathrm{s}'}}f_{\mathrm{s}}{}^{\mathbf{j}}\frac{\delta f_{\mathrm{s}'}{}^{\mathbf{k}}}{\delta\mathbf{u}'}\right)\Delta\mathbf{u}'\right]\Delta\mathbf{u} \\ &= -\frac{\Gamma}{2}\sum_{\mathbf{j},\mathbf{k}}\left[\mathsf{U}(\mathbf{u}^{\mathbf{j}},\mathbf{u}'^{\mathbf{k}})\cdot\frac{\delta(\gamma^{\mathbf{j}}c^2)}{\delta\mathbf{u}}\cdot\left(\frac{f_{\mathrm{s}'}{}^{\mathbf{k}}}{m_{\mathrm{s}}}\frac{\delta f_{\mathrm{s}}{}^{\mathbf{j}}}{\delta\mathbf{u}} - \frac{f_{\mathrm{s}}{}^{\mathbf{j}}}{m_{\mathrm{s}'}}\frac{\delta f_{\mathrm{s}'}{}^{\mathbf{k}}}{\delta\mathbf{u}'}\right)\right]\Delta\mathbf{u}\Delta\mathbf{u}'.\end{aligned} \tag{13}$$

Likewise, the energy of species "s′" is obtained as follows:

$$\frac{\partial}{\partial t}\left(\sum_{\mathbf{k}} m_{\mathrm{s}'}c^2\gamma'^{\mathbf{k}} f_{\mathrm{s}'}{}^{\mathbf{k}}\Delta\mathbf{u}'\right) = -\frac{\Gamma}{2}\sum_{\mathbf{j},\mathbf{k}}\left[\mathsf{U}(\mathbf{u}'^{\mathbf{k}},\mathbf{u}^{\mathbf{j}})\cdot\frac{\delta(\gamma'^{\mathbf{k}}c^2)}{\delta\mathbf{u}'}\cdot\left(\frac{f_{\mathrm{s}}{}^{\mathbf{j}}}{m_{\mathrm{s}'}}\frac{\delta f_{\mathrm{s}'}{}^{\mathbf{k}}}{\delta\mathbf{u}'} - \frac{f_{\mathrm{s}'}{}^{\mathbf{k}}}{m_{\mathrm{s}}}\frac{\delta f_{\mathrm{s}}{}^{\mathbf{j}}}{\delta\mathbf{u}}\right)\right]\Delta\mathbf{u}'\Delta\mathbf{u}. \tag{14}$$

The temporal development of total energy is obtained as a sum of Eqs. (13) and (14):

$$\frac{\partial}{\partial t}\left(\sum_{\mathbf{j}} m_{\mathrm{s}}c^2\gamma^{\mathbf{j}} f_{\mathrm{s}}{}^{\mathbf{j}}\Delta\mathbf{u} + \sum_{\mathbf{k}} m_{\mathrm{s}'}c^2\gamma'^{\mathbf{k}} f_{\mathrm{s}'}{}^{\mathbf{k}}\Delta\mathbf{u}'\right) = -\frac{\Gamma}{2}\sum_{\mathbf{j},\mathbf{k}}\left\{[\mathsf{U}(\mathbf{u}^{\mathbf{j}},\mathbf{u}'^{\mathbf{k}})\cdot\bar{\mathbf{v}} - \mathsf{U}(\mathbf{u}'^{\mathbf{k}},\mathbf{u}^{\mathbf{j}})\cdot\bar{\mathbf{v}}']\cdot\left(\frac{f_{\mathrm{s}'}{}^{\mathbf{k}}}{m_{\mathrm{s}}}\frac{\delta f_{\mathrm{s}}{}^{\mathbf{j}}}{\delta\mathbf{u}} - \frac{f_{\mathrm{s}}{}^{\mathbf{j}}}{m_{\mathrm{s}'}}\frac{\delta f_{\mathrm{s}'}{}^{\mathbf{k}}}{\delta\mathbf{u}'}\right)\right\}\Delta\mathbf{u}\Delta\mathbf{u}', \tag{15}$$

where the velocities with overlines are defined as follows:

$$\bar{\mathbf{v}} \equiv \frac{\delta(\gamma^{\mathbf{j}}c^2)}{\delta\mathbf{u}}, \quad \bar{\mathbf{v}}' \equiv \frac{\delta(\gamma'^{\mathbf{k}}c^2)}{\delta\mathbf{u}'}. \tag{16}$$

Therefore, $\mathsf{U}(\mathbf{u}^{\mathbf{j}},\mathbf{u}'^{\mathbf{k}})\cdot\bar{\mathbf{v}} = \mathsf{U}(\mathbf{u}'^{\mathbf{k}},\mathbf{u}^{\mathbf{j}})\cdot\bar{\mathbf{v}}'$ is required for the energy conservation in discrete form. The intuitive kernel

Eq. (7) satisfies $\mathsf{U}(\mathbf{u}^{\mathbf{j}}, \mathbf{u}'^{\mathbf{k}}) \cdot \mathbf{v}^{\mathbf{j}} = \mathsf{U}(\mathbf{u}'^{\mathbf{k}}, \mathbf{u}^{\mathbf{j}}) \cdot \mathbf{v}'^{\mathbf{k}}$ rather than $\mathsf{U}(\mathbf{u}^{\mathbf{j}}, \mathbf{u}'^{\mathbf{k}}) \cdot \bar{\mathbf{v}} = \mathsf{U}(\mathbf{u}'^{\mathbf{k}}, \mathbf{u}^{\mathbf{j}}) \cdot \bar{\mathbf{v}}'$, so the energy conservation would be preserved even in discrete form if $\bar{\mathbf{v}} = \mathbf{v}^{\mathbf{j}}$ and $\bar{\mathbf{v}}' = \mathbf{v}'^{\mathbf{k}}$ were true. Generally speaking, the proposition is false resulting in a violation of the energy conservation with the intuitive scheme. For the second-order central difference,

$$(\gamma^{j_1+1,j_2,j_3})^2 - (\gamma^{j_1-1,j_2,j_3})^2 = ({u_1}^{j_1+1}/c)^2 - ({u_1}^{j_1-1}/c)^2,$$

$$\therefore \bar{v}_1 = \frac{\delta(\gamma^{\mathbf{j}} c^2)}{\delta u_1} = \frac{2{u_1}^{j_1}}{\gamma^{j_1+1,j_2,j_3} + \gamma^{j_1-1,j_2,j_3}} \neq \frac{{u_1}^{j_1}}{\gamma^{j_1,j_2,j_3}}.$$

The only exception is the nonrelativistic limit when the Lorentz factor is always unity. Hirvijoki and Adams reported that their scheme cannot maintain the exact energy conservation in the relativistic regime [30], and our discussion should be connected on the fundamental level with this issue although their discussion was based on the finite-element method.

IV. STRUCTURE-PRESERVING STRATEGY

Here we propose a structure-preserving scheme for the relativistic LFP equation which resolves the energy-conservation problem of the intuitive scheme. According to Eqs. (12) and (15), the analytical requirements shown at the beginning of Sec. III must be modified in discrete form as follows:

(1) Summation-by-parts
(2) $\mathsf{U}(\mathbf{u}^{\mathbf{j}}, \mathbf{u}'^{\mathbf{k}}) = \mathsf{U}(\mathbf{u}'^{\mathbf{k}}, \mathbf{u}^{\mathbf{j}})$
(3) $\mathsf{U}(\mathbf{u}^{\mathbf{j}}, \mathbf{u}'^{\mathbf{k}}) \cdot \bar{\mathbf{v}} = \mathsf{U}(\mathbf{u}'^{\mathbf{k}}, \mathbf{u}^{\mathbf{j}}) \cdot \bar{\mathbf{v}}'$

The following is the only Beliaev-Budker kernel that preserves the above requirements:

$$\mathsf{U}(\mathbf{u}^{\mathbf{j}}, \mathbf{u}'^{\mathbf{k}}) \equiv \frac{\bar{r}^2}{\bar{\gamma}\bar{\gamma}'\bar{w}^3}[\bar{w}^2 \mathsf{I} - \bar{\gamma}^2 \bar{\mathbf{v}}\bar{\mathbf{v}} - \bar{\gamma}'^2 \bar{\mathbf{v}}'\bar{\mathbf{v}}' + \bar{r}\bar{\gamma}\bar{\gamma}'(\bar{\mathbf{v}}\bar{\mathbf{v}}' + \bar{\mathbf{v}}'\bar{\mathbf{v}})], \tag{17}$$

where the variables with overlines are

$$\bar{\gamma} \equiv 1/\sqrt{1 - |\bar{\mathbf{v}}/c|^2} \neq \gamma^{\mathbf{j}}, \quad \bar{\gamma}' \equiv 1/\sqrt{1 - |\bar{\mathbf{v}}'/c|^2} \neq \gamma'^{\mathbf{k}},$$
$$\bar{r} \equiv \bar{\gamma}\bar{\gamma}'(1 - \bar{\mathbf{v}} \cdot \bar{\mathbf{v}}') \neq r^{\mathbf{j},\mathbf{k}}, \quad \bar{w} \equiv c\sqrt{\bar{r}^2 - 1} \neq w^{\mathbf{j},\mathbf{k}}.$$

A combination of Eqs. (6) and (17) preserves the law of energy conservation naturally. However, the positivity of distribution function and H-theorem are not guaranteed unconditionally by this formulation. We do not give a discussion of the temporal discretization in this article, which is done in the papers about entropic schemes.

V. DEMONSTRATION

To verify the proposed scheme, a collisional relaxation of a particle-antiparticle plasma is calculated for simplicity ($m_s = m_{s'} \equiv m, q_s = -q_{s'} \equiv q$). The particles (species "s") and antiparticles (species "s'") are initialized by the following shifted Maxwell-Jüttner distrubtions [42].

$$f_s(\mathbf{u}) = \exp\left(-\frac{\gamma - 1}{\theta}\right),$$
$$f_{s'}(\mathbf{u}') = \frac{1}{\gamma_0}\exp\left(-\frac{\gamma'\gamma_0 - \gamma_0 \mathbf{v}_0 \cdot \mathbf{u}'/c^2 - 1}{\theta}\right),$$

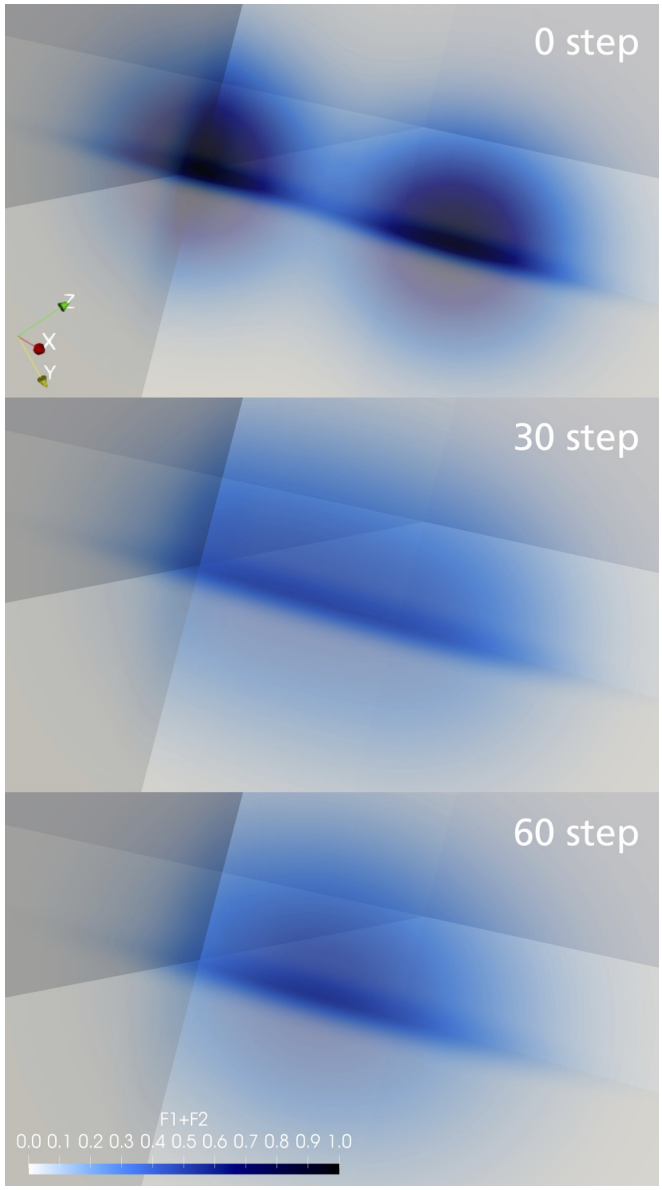

FIG. 1. Time development of distribution function initialized by double Maxwell-Jüttner distribution.

where $\theta = 0.01$ is the temperature normalized by the rest mass energy, $\mathbf{v}_0/c = [0.2, 0.2, 0.2]$, and $\gamma_0 = 1/\sqrt{1 - \mathbf{v}_0 \cdot \mathbf{v}_0/c^2}$. The computational domain is set to be $\{(u_1, u_2, u_3) | -1.2c \leqslant u_1, u_2, u_3 \leqslant 1.8c\}$, and the number of computational cells is $128 \times 128 \times 128$. In this verification, a first-order Euler explicit method is used as a time integration. The temporal interval is given as $\Gamma m^{-2}\Delta t = 1/80$, so that the temporal resolution is fine enough to see the relaxation. In this test, only an unlike-particle collision is considered since it is the least element of multispecies collisions.

Figure 1 shows a time development of the double Maxwell-Jüttner distribution through the collisional relaxation. The double-peaked distribution function approximates to the equilibrium state whose velocity shift and temperature are $\mathbf{v}_0/2$ and 2θ, respectively. Figure 2 indicates the errors of conservation laws for the structure-preserving and intuitive

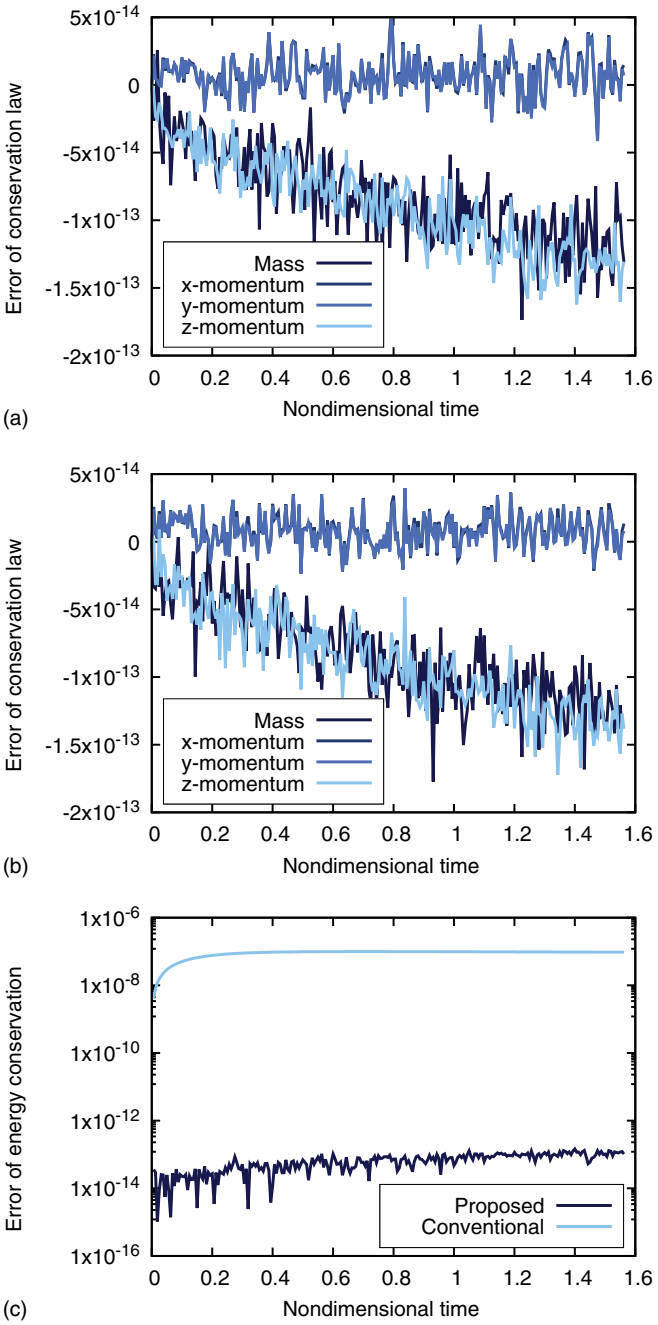

FIG. 2. Conservation errors for mass, momentum, and energy in a thermal-equilibration verification. (a) Structure-preserving discretization (proposed), (b) Intuitive discretization (conventional), and (c) Comparison of energy conservation property.

discretizations, respectively. Here we use a nondimensional time normalized by the collision time ($\tau \equiv \Gamma m^{-2} t/2$). As shown in Figs. 2(a) and 2(b), both schemes strictly maintain the conservation laws of mass and momentum. It seems that some of the conservative quantities slightly accumulate the round-off errors. We reported that Padé-type (or implicit) filters used in computational fluid dynamics can accumulate round-off errors, but it can be suppressed by changing the order of arithmetic operations [43]. Therefore, the accumulation of round-off errors can be resolved by an optimization of the

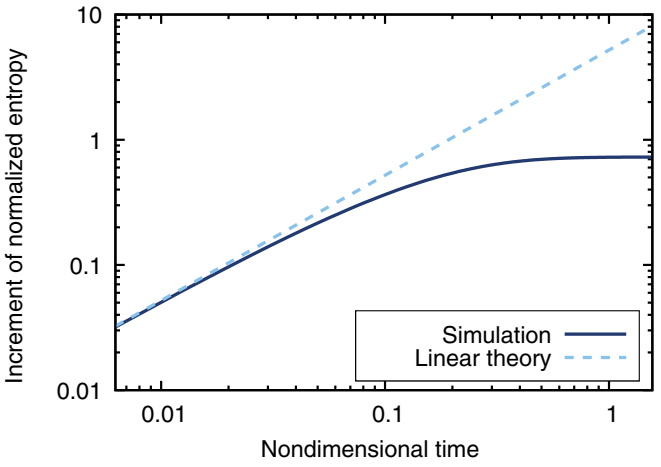

FIG. 3. Verification of H-theorem. Caution: the proposed scheme does not ensure the H-theorem mathematically.

code, although it is out of the scope of this article. From the other perspective, the conservation property is quite fine as well as it is affected by the order of arithmetic operations. In contrast, these schemes show clearly different trends at the point of energy conservation: Fig. 2(c) indicates that the structure-preserving scheme strictly maintains the energy conservation while the conventional scheme has much greater error than the round-off level. Therefore, it has been numerically demonstrated that the structure-preserving strategy is required to maintain the energy conservation in the relativistic LFP simulations.

Finally, we address some remaining issues about the positivity and H-theorem. Figure 3 shows the H-theorem is strictly preserved and the linear relaxation rate is initially reproduced well in the current situation. Here we introduced the entropy as follows to avoid negative values due to round-off errors:

$$S \equiv -\sum_{\mathbf{j}} \left|f_s^{\mathbf{j}}\right| \log \left|f_s^{\mathbf{j}}\right| \Delta\mathbf{u} - \sum_{\mathbf{k}} \left|f_{s'}^{\mathbf{k}}\right| \log \left|f_{s'}^{\mathbf{k}}\right| \Delta\mathbf{u}'.$$

The linear relaxation rate is obtained as follows by assuming the initial Maxwellian:

$$\left(\frac{\Gamma}{2m^2}\right)^{-1} \frac{1}{S(0)} \frac{\mathrm{d}S}{\mathrm{d}t} \simeq 5.2.$$

Reference [32], for example, suggests that there is an upper bound of Δt which ensures the positivity and H-theorem. In this experiment, the collision time is resolved quite well so that the requirement is satisfied. However, such a small temporal interval is not suited for practical simulations. We did not have a discussion about the temporal discretization in this article since the conservation laws do not depend on the temporal structure of the relativistic LFP equation. A development of conservative and entropic scheme for the relativistic LFP equation will be performed in the separate paper.

VI. CONCLUSIONS

The feasibility of a conservative scheme for the relativistic Landau-Fokker-Planck equation has been demonstrated. The proposed scheme has a unique way of calculating the

Beliaev-Budker kernel specialized for linear finite-difference operators. The verification via the thermal-equilibration problem manifests the conservation of mass, momentum, and energy only with round-off errors. Although there are still some problems of computational cost, positivity, H-theorem, and boundary conditions, our strategy gives a piece of puzzle for practical simulation of the collisional relaxation in the relativistic regime.

ACKNOWLEDGMENTS

T.S. would like to appreciate valuable information from Dr. William T. Taitano and Dr. Luis Chacón (Los Alamos National Laboratory). This work was supported by KAKENHI Grants No. 15K21767 and No. 18H05851. Numerical experiments were carried out on NEC SX-ACE, Cybermedia Center, Osaka University.

[1] M. Tabak, J. Hammer, M. E. Glinsky, W. L. Kruer, S. C. Wilks, J. Woodworth, E. M. Campbell, M. D. Perry, and R. J. Mason, Ignition and high gain with ultrapowerful lasers, Phys. Plasmas **1**, 1626 (1994).

[2] H. Dreicer, Electron and ion runaway in a fully ionized gas. I, Phys. Rev. **115**, 238 (1959).

[3] M. N. Rosenbluth and S. V. Putvinski, Theory for avalanche of runaway electrons in tokamaks, Nucl. Fusion **37**, 1355 (1997).

[4] E. Fermi, On the origin of the cosmic radiation, Phys. Rev. **75**, 1169 (1949).

[5] E. M. Lifshitz and L. P. Pitaevskii, *Physical Kinetics* (Pergamon Press, Oxford, 1981).

[6] S. T. Beliaev and G. I. Budker, The relativistic kinetic equation, Sov. Phys. Dokl. **1**, 218 (1956).

[7] K. Nakashima and H. Takabe, Numerical study of pair creation by ultraintense lasers, Phys. Plasmas **9**, 1505 (2002).

[8] T. Yokota, Y. Nakao, T. Johzaki, and K. Mima, Two-dimensional relativistic Fokker–Planck model for core plasma heating in fast ignition targets, Phys. Plasmas **13**, 022702 (2006).

[9] T. Johzaki, Y. Nakao, and K. Mima, Fokker–Planck simulations for core heating in subignition cone-guiding fast ignition targets, Phys. Plasmas **16**, 062706 (2009).

[10] M. Sherlock, Universal scaling of the electron distribution function in one-dimensional simulations of relativistic laser-plasma interactions, Phys. Plasmas **16**, 103101 (2009).

[11] C. P. Ridgers, M. Sherlock, R. G. Evans, A. P. L. Robinson, and R. J. Kingham, Superluminal sheath-field expansion and fast-electron-beam divergence measurements in laser-solid interactions, Phys. Rev. E **83**, 036404 (2011).

[12] C. F. F. Karney and N. J. Fisch, Efficiency of current drive by fast waves, Phys. Fluids **28**, 116 (1985).

[13] C. F. F. Karney, Fokker–Planck and quasilinear codes, Comput. Phys. Rep. **4**, 183 (1986).

[14] H. Nuga, M. Yagi, and A. Fukuyama, Fokker-Planck simulation of runaway electron generation in disruptions with the hot-tail effect, Phys. Plasmas **23**, 062506 (2016).

[15] H. Nuga and A. Fukuyama, Kinetic integrated modeling of plasma heating in tokamaks, in *Progress in Nuclear Science and Technology*, Vol. 2 (Atomic Energy Society of Japan, 2011), pp. 78–84.

[16] Y. V. Petrov and R. W. Harvey, A fully-neoclassical finite-orbit-width version of the CQL3D Fokker–Planck code, Plasma Phys. Controlled Fusion **58**, 115001 (2016).

[17] A. Stahl, M. Landreman, O. Embréus, and T. Fülöp, NORSE: A solver for the relativistic non-linear Fokker–Planck equation for electrons in a homogeneous plasma, Comput. Phys. Commun. **212**, 269 (2017).

[18] B. J. Braams and C. F. F. Karney, Differential form of the Collision Integral for a Relativistic Plasma, Phys. Rev. Lett. **59**, 1817 (1987).

[19] W. T. Taitano, L. Chacón, A. N. Simakov, and K. Molvig, A mass, momentum, and energy conserving, fully implicit, scalable algorithm for the multi-dimensional, multi-species Rosenbluth–Fokker–Planck equation, J. Comput. Phys. **297**, 357 (2015).

[20] W. T. Taitano, L. Chacón, and A. N. Simakov, An equilibrium-preserving discretization for the nonlinear Rosenbluth–Fokker–Planck operator in arbitrary multi-dimensional geometry, J. Comput. Phys. **339**, 453 (2017).

[21] E. Eich, Convergence Results for a coordinate projection method applied to mechanical systems with algebraic constraints, SIAM J. Numer. Anal. **30**, 1467 (1993).

[22] J. U. Brackbill and D. C. Barnes, The effect of monzero $\nabla \cdot \mathbf{B}$ on the numerical solution of the magnetohydrodynamic equations, J. Comput. Phys. **35**, 426 (1980).

[23] C. R. Evans and J. F. Hawley, Simulation of magnetohydrodynamic flows: A constrained transport method, Astrophys. J. **332**, 659 (1988).

[24] M. Flock, N. Dzyurkevich, H. Klahr, and A. Mignone, High-order Godunov schemes for global 3D MHD simulations of accretion disks: I. Testing the linear growth of the magneto-rotational instability, Astron. Astrophys. **516**, A26 (2010).

[25] J. S. Chang and G. Cooper, A practical difference scheme for Fokker–Planck equations, J. Comput. Phys. **6**, 1 (1970).

[26] C. Buet and S. Cordier, Numerical analysis of the isotropic Fokker–Planck–Landau equation, J. Comput. Phys. **179**, 43 (2002).

[27] E. S. Yoon and C. S. Chang, A Fokker–Planck–Landau collision equation solver on two-dimensional velocity grid and its application to particle-in-cell simulation, Phys. Plasmas **21**, 032503 (2014).

[28] E. S. Yoon and C. S. Chang, Erratum: "A Fokker–Planck–Landau collision equation solver on two-dimensional velocity grid and its application to particle-in-cell simulation" [Phys. Plasmas 21, 032503 (2014)], Phys. Plasmas **21**, 039905 (2014).

[29] R. Hager, E. S. Yoon, S. Ku, E. F. D'Azevedo, P. H. Worley, and C. S. Chang, A fully non-linear multi-species Fokker–Planck–Landau collision operator for simulation of fusion plasma, J. Comput. Phys. **315**, 644 (2016).

[30] E. Hirvijoki and M. F. Adams, Conservative discretization of the Landau collision integral, Phys. Plasmas **24**, 032121 (2017).

[31] M. S. Pekker and V. N. Khudik, Conservative difference schemes for the Fokker–Planck equation, USSR Comput. Math. Math. Phys. **24**, 206 (1984).

[32] Y. A. Berezin, V. N. Khudik, and M. S. Pekker, Conservative finite-difference schemes for the Fokker–Planck equation not violating the law of an increasing entropy, J. Comput. Phys. **69**, 163 (1987).

[33] C. Buet and S. Cordier, Conservative and entropy decaying numerical scheme for the isotropic Fokker–Planck–Landau equation, J. Comput. Phys. **145**, 228 (1998).

[34] P. Degond and B. Lucquin-Desreux, An entropy scheme for the Fokker–Planck collision operator of plasma kinetic theory, Numer. Math. **68**, 239 (1994).

[35] C. Buet, S. Cordier, P. Degond, and M. Lemou, Fast algorithm for numerical, conservative, and entropy approximations of the Fokker–Planck–Landau equation, J. Comput. Phys. **133**, 310 (1997).

[36] M. N. Rosenbluth, W. M. MacDonald, and D. L. Judd, Fokker–Planck equation for an inverse-square force, Phys. Rev. **107**, 1 (1957).

[37] L. Chacón, D. C. Barnes, D. A. Knoll, and G. H. Miley, An implicit energy-conservative 2D Fokker–Planck algorithm: I. Difference scheme, J. Comput. Phys. **157**, 618 (2000).

[38] L. Chacón, D. C. Barnes, D. A. Knoll, and G. H. Miley, An implicit energy-conservative 2D Fokker–Planck algorithm: II. Jacobian-free Newton–Krylov solver, J. Comput. Phys. **157**, 654 (2000).

[39] T. Shiroto, N. Ohnishi, and Y. Sentoku, Quadratic conservative scheme for relativistic Vlasov–Maxwell system, J. Comput. Phys. **379**, 32 (2019).

[40] C. Buet and K.-C. Le Thanh, About positive, energy conservative and equilibrium state preserving schemes for the isotropic Fokker–Planck–Landau equation, hal-00092543 (2006), https://hal.archives-ouvertes.fr/hal-00092543/.

[41] C. Buet and K.-C. Le Thanh, Positive, conservative, equilibrium state preserving and implicit difference schemes for the isotropic Fokker–Planck–Landau equation, hal-00142408 (2007), https://hal.archives-ouvertes.fr/hal-00142408v3.

[42] S. Zenitani, Loading relativistic Maxwell distributions in particle simulations, Phys. Plasmas **22**, 042116 (2015).

[43] T. Shiroto, S. Kawai, and N. Ohnishi, Finite-volume-concept-based Padé-type filters, J. Comput. Phys. **349**, 215 (2017).